RJC

RASĀYAN *J. Chem.*
Vol. 14 | No. 1 |466-472| January - March | 2021
ISSN: 0974-1496 | e-ISSN: 0976-0083 | CODEN: RJCABP
http://www.rasayanjournal.com
http://www.rasayanjournal.co.in

MORPHOLOGY OF BARITE PRECIPITATED FROM INDUCED FLOW VIBRATION AND THE PRESENCE OF CHEMICAL ADDITIVES

N. Karaman[1], W. Mangestiyono[2], S. Muryanto[3], J. Jamari[4] and A.P. Bayuseno[4,✉]

[1]Department of Chemical Engineering, Universitas Pembangunan Nasional Veteran, Surabaya, Indonesia
[2]Mechanical Engineering, School of Vocational, Diponegoro University, Semarang, Indonesia
[3]Department of Chemical Engineering, UNTAG University, Semarang, Indonesia
[4]Department of Mechanical Engineering, Diponegoro University, Semarang, Indonesia
✉Corresponding Author: apbayuseno@gmail.com

ABSTRACT

Crystallization of barite ($BaSO_4$) in industrial processes has been intensively investigated for the production of fine particles. In this way, crystallite size and morphology are important characteristics determining the quality product of barite. The effects of the mechanical vibration and the presence of chemical additives in the solution chemistry on the properties of barite particles were examined in this study. Barite crystal was formed through the experiments of the vibrated pipes of water flowing and adding chemical additives (formic, tartaric, oxalic, and acetic acids). The crystal morphology of barite in the different crystallographic directions corresponding to the X-ray diffraction (XRD) patterns was examined. Here, barite morphology with rosettes was predominantly observed by SEM. The study demonstrated that barite with nano-crystalline was successfully precipitated from the chemistry solution. Barite particles gradually decreased in size when crystallographic planes increased with 2θ-values. No significant variation of barite crystal morphologies was found, but rosette- fine crystals might transform into granular nano-crystals when induced by vibration. Importantly, the mechanical vibration and chemical additives with acids in the solution chemistry influenced the morphology of barite. In practical terms, the induced mechanical vibration and the added acids could be an important unit operation for the production of barite with controlled morphology.

Keywords: Crystallization of Barite, Chemical Additives, Vibrated Pipes, XRD Analysis, SEM Analysis.

RASĀYAN *J. Chem.*, Vol. 14, No.1, 2021

INTRODUCTION

Barite ($BaSO_4$) is an important mineral having good stability and is abundantly formed as Earth deposits. Instead, the barite formation has been widely investigated to provide knowledge of the origin of the formation of barite deposits. Additionally, It can be used for distinguishing abiotic and biology factors influencing precipitation of barite.[1-4] Correspondingly, this understanding of the specific geochemical and morphological features in a marine ecosystem such as salinity and ocean currents may describe the non-living resource productivity affecting a living organism.[5,6]

Further, barite morphology developed in the marine ecosystem was reported to have a shape (sub-spherical or elliptical like-crystals) with uniform size of submicron to 5 μm and can be found on the pelagic barite crystals resulting from the nucleation and crystal growth at a very stable condition. Moreover, barite crystals with ovoid and hexagonal-shaped-like morphology are commonly found on the biotic forms of pelagic barite.[7-11] However, barite crystal morphologies resulting from the hydrothermal environment are commonly formed in shapes with tabular, acicular/radiating tapered and bladed to dendritic.[7,8,12,13] Here, the cross-cutting tabular crystals may be formed from rosette structures in the hydrothermal and cold seep barite (sub-spherical, elliptical crystals) (subspherical, elliptical crystals)[14-16], whereas diagenesis of barite may result in thick or thin tabular crystals[17,18] or bladed in cluster layers.[17]

Furthermore, there may be barite with varying morphologies of crystals (e.g. dendrite and rosette) growing in the modern continental warm springs.[10,19] Here abiotic factors such as atmosphere, chemical

http://dx.doi.org/10.31788/ RJC.2021.1415892

elements, sunlight/temperature, wind, and water may control the variation of barite crystal morphologies forming on continental spring conditions. Correspondingly, the morphology of barite with euhedral platy-shape may precipitate at the liquid-liquid interfaces and solutions with high ionic strength, while supersaturated solutions and water-air interfaces may produce stellate barite form.[1] Likewise, barite with euhedral, tabular, and rhombic morphologies may be formed at the liquid. Conversely, barite having subhedral and anhedral microcrystals may be precipitated from the solution with microorganism.[1]

Since much previous research of barite formation has been performed in natural environments, on which several conditions may influence the yield of morphology, it may be questioned to evaluate the effect of process parameters on a specific crystal morphology under influence of industrial crystallization. In this regard, barite formation could be implemented in industrial crystallization to produce fine solids, such as catalysts, pigments, and pharmaceuticals. In particular, crystallization of barite may include varying mass transfer quantities in supersaturated solutions. Accordingly, this process depends upon solution temperature, supersaturation, mixing speed, and the presence of chemical additives, whereas the most significant effect of the crystallization process is the presence of chemical additives.[20,21] Additionally, barite could be precipitated as scale in many industrial and oil drilling processes,[22,23] on which the insoluble scales are produced to make it difficult to detach[24]. Thus for the control of particle products in industrial crystallization, the crystal growth and morphological changes of the crystal are desired,[25] and here chemical additives are often employed in industrial crystallization to control the nucleation, growth behavior, size, and morphology of crystals.[26] Correspondingly, a well-controlled experimental setting is required for examining individually the effect of each parameter on the yield of morphology.

Many experimental efforts were attempted for investigating the nucleation and growth mechanisms of barite formed in the hydrothermal solution.[9,11,27,28] Here dominant factors influencing barite crystal morphology may include the chemical composition of the liquid, rate diffusion of molecules, and crystallization rate.[9,11,29] Here barite with dendritic/irregular crystals was proposed for the result of the limited crystal growth rate.[28] Moreover,several factors such as saturated solution[21], Ba^{2+}/SO_4^{2-} ratio,[27,30-32], mixing rate[27,28], temperature[27, 28, 33] and presence of organic compounds in the solution[34,35] may control barite crystal morphology. Similarly, the humid condition may control the crystallization and morphology of barite.[36,37] Also, organic compounds hamper the spontaneous crystallization of barite. These organic substances inhibiting the crystallization of barite by absorbing them on the crystal surfaces[37], which may protect the substrate from other ions to form mineral phases.[38,39] Significantly, changes in crystal morphology of barite may be related to the reaction parameters, which can be explored from varying intensities of XRD (x-ray diffraction) peaks. Also, this condition may relate to the crystal habit. In this way, the morphology of barite can be explored from the full-width half maximum (FWHM) of x-ray intensity. However, a limited study can be found in literature, which presents data correlating of barite morphology and XRD peak, while the experimental data are needed to control the barite morphology during the crystallization process. Also, there are no previous published works of barite crystal formation under the influence of mechanical vibration on a pipe and the presence of chemical additives.

In this paper, barite crystal morphologies resulting from the solution chemistry under influence of the vibrated piping system and chemical additives were performed. Six major diffraction peaks: (200), (210), (211), (020), (401) and (410) were examined in the study. These selected peaks have strong XRD intensities, while other diffraction peaks were negligibly low. Barite crystals were synthesized from induced vibrated solutions with appropriate concentrations without additives. Morphology of precipitated barite examined by scanning electron microscope (SEM). The resulting experimental data may add knowledge on the control of barite morphology precipitated from the induced flow vibration.

EXPERIMENTAL

Material and Methods

For crystallization experiments of barite, $BaCl_2$ and Na_2SO_4 solutions were prepared by which 3500 ppm concentration of each in 50 ml volume was predetermined. In every experiment, the sulphate solution was added to a small amount (0, 5, and 10 ppm) of each acid separately. The experimental works were conducted at room temperature. The pump circulates the solution at a rate of 30 ml/min. The crystallization process of barite within the metallic coupon was subjected to mechanical vibration (4.00

and 8.00 Hz). In this present research, barite morphologies were generated by reaction crystallization of induced flow vibration with chemical additives, which are formic (CH_2O_2), tartaric ($C_4H_6O_6$), oxalic ($C_2H_2O_4$), and acetic ($C_2H_4O_2$) acids. The detailed experimental apparatus is shown elsewhere.[40] After 4 h-working duration, the experiment was stopped, while the barite powder deposited on the metallic coupon was removed and dried at a temperature of 60 ^{O}C for 6 h. Later, the dried powders were subjected to X-ray (Rint-Ultima III, Rigaku Diffractometer) and SEM/EDX examinations.

Analytical Discussion

This study mainly examined the effects of mechanical vibration and organic additive on the crystallization of barite and its impact on the crystal morphology of barite and varying crystallite sizes of each crystal face (*hkl*). In this way, the XRD data containing peak positions and peak intensity was initially matched with the ICDD-PDF database (the International Centre for Diffraction Data-Powder Diffraction File). Subsequently, the matched phases were verified by the Rietveld method (FullProf-2k software version 3.30), using the well-known crystal structure model obtained from the American mineralogist crystal structure database (AMCSD). Specifically, crystallite size along with the direction perpendicular to the lattice plane (*hkl*) was computed related to the strongest refined XRD peaks. Also, the morphology of barite was observed by SEM (scanning electron microscope (FEI Inspect S50). Finally, the morphology related to the XRD intensity was analyzed and discussed.

RESULTS AND DISCUSSION

Barite Morphology in the Presence of Vibration and Additives

The FWHM of peaks on (200), (210), (211), (020), (401) and (410) was investigated to relate the change of morphology in the presence of additives. Especially, the FWHM of (200) and (401) peaks were selected because of having strong intensity. Therefore, the influence of vibration and chemical additives on crystal morphology are investigated by the XRD analysis in this section. Experimental results of crystallite size obtained from the exploration of XRD peaks for all samples are shown in Fig.-1, while SEM micrographs of those samples are shown in Fig.-2.

The X-ray powder diffraction analyses were performed on the obtained-six barite samples from the crystallization with no-inhibitors and no-vibration; no inhibitors and with vibration; with inhibitors and induced vibration respectively (Fig.-1). Based on the XRD Rietveld analysis, the pure barite was only developed in the precipitating solid; while there were no significant variations in the intensity of XRD peaks. Particularly, the rosette crystals (Fig.-2) have become a dominant morphology of barite; however, an irregular rosette with platy crystals (Fig.-2a) matched for the precipitated barite without additives and vibration, on which well-rounded and spherical crystals were found in the SEM image. When compared to barite morphology precipitated from the vibrated solution and additives, more regular rosette crystals with dense structures were developed during the experiments (Fig.-2b to e). This might have occurred because the vibration may contribute to the hydrodynamic force leading to precipitate with well-regular rosette crystals. In particular, a developed regular rosette crystal can be found on the barite obtained from vibrated solution without additive (Fig.-2f). These results agreed very well with the data of the previous research[18].

Further effects of acids and the mechanical vibration were significant on barite crystallization through changing parts of the chemical reaction mechanism in the solution[41]. Consequently, barite had the dominant rosette-like crystal surfaces, which may differ significantly without induced vibration, because of the abundance of S atom compared to the Ba atom in $BaSO_4 \cdot 2H_2O$ crystal (Fig.-2b to f). These results suggested that the position of Ba atoms may be at the center of the rosette form for barite morphology. This condition would be more likely to occur in the presence of vibration. Apparently, barite would grow along the longitude direction and suppress in the presence of acids, on which ions of additives and Ba atoms would interact electrostatically at the position of the lattice of rosette crystals. This condition made shape changes by suppressing surfaces for growing, consequently, the size of the barite crystals would reduce. The use of polyelectrolytes having carboxyl groups is proposed for changing on shape and size of crystals simultaneously. Here the crystal shapes changing from rosette or plate into granular could be possible. When no electrostatic interaction between additives with $BaSO_4 \cdot 2H_2O$ crystal is making

additives be adsorbed equally to each surface of the crystal, which results in the change of their crystal shape.

Further, the dominant rosette structure was obvious from the precipitation experiments of barite during the study (Table-1). Additionally, the use of Scherrer equation[35] for determining sizes of crystal barite related to selected intensity peaks, on which the FWHMs of each diffraction peak corresponding to (hkl) planes were determined. The apparent crystallite size of the barite is presented in Table-1. In this method of line broadening contribution due to the crystallites size is taken into consideration. A gradual decrease in crystallite size (20-70 Å) was observed for barite crystals with varying (*hkl*) planes. The microstructure of the powder prepared by the precipitation process is observed by SEM that there is a distribution of small particles and large agglomerates. Correspondingly, the insignificant distribution of crystallite size with diffraction peaks indicates the crystallization process resulting in the homogeneity of the powder, which can be precipitated from the induced vibrated solution.

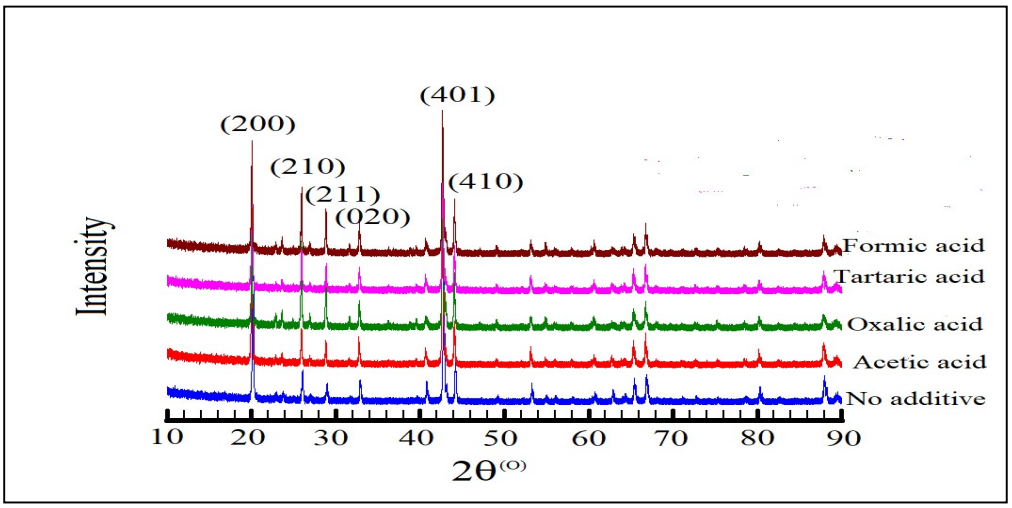

Fig.-1: XRD Charts of all Samples resulted from the 8-Hz Vibrated Solution without and with Acids (10 ppm) indicating the Strong Intensities on the Crystallographic Planes (*hkl*)

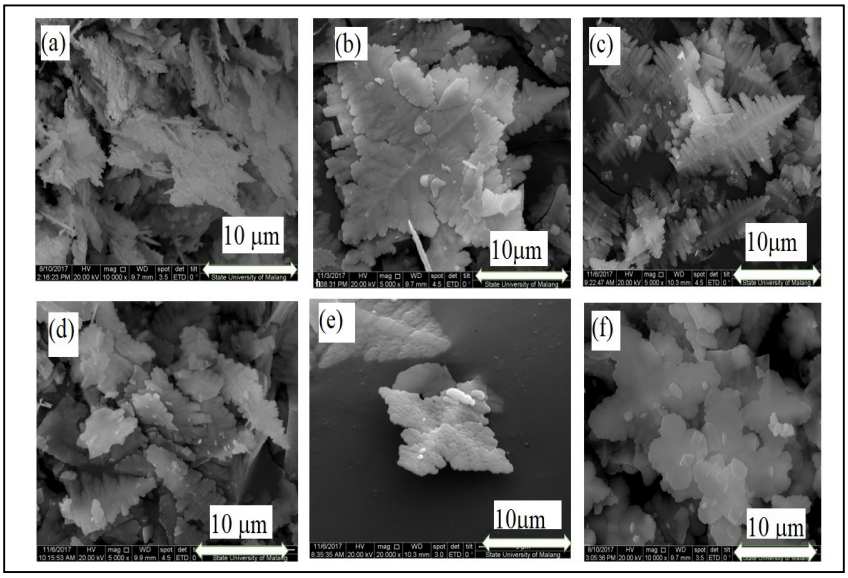

Fig.-2: SEM Micrographs of Barite Morphologies obtained from the Experiments of; (a) without acids and vibrated condition; (b) 8 Hz of induced vibration with 10 ppm acetic acid; (c) 8 Hz of induced vibration with 10 ppm oxalic acid; (d) 8 Hz of induced vibration tartaric acid; (e) 8 Hz of induced vibration with 10 ppm formic acid; (f) 8 Hz of induced vibration and without acids

However, further experimental work should be done to examine the crystallization mechanism at varying frequency vibrations. Also, an experiment with solutions containing other ions of Ca, Mg, and Sr may provide varying morphologies of barite.[43,44] Here barite crystal structure may incorporate one of these ions leading to crystal growth rate changing at different faces. Moreover to determine the barite morphology can relate to step kinetics. In the orthorhombic crystal system, barite crystal changes in shape due to these ion incorporation corresponding to the growth rate in the specific crystallographic direction.[43,44]

Table-1: Experimental Results of Barite Crystal (Crystal Morphology and Crystal Size)

Sample	$2\theta^{O}$	FWHM	(hkl)	Crystallite Size (Å)	Crystal morphology
No additive- no vibrated condition	19.976	0.194	(200)	42.80	Rosettes
	25.852	0.183	(210)	35.06	Rosettes
	28.750	0.178	(211)	32.41	Rosettes
	32.824	0.171	(020)	29.55	Rosettes
	42.595	0.158	(401)	24.65	Rosettes
	43.993	0.157	(410)	24.02	Rosettes
vibrated at 8 Hz without additive	19.970	0.123	(200)	67.53	Rosettes
	25.850	0.12	(210)	53.48	Rosettes
	28.747	0.119	(211)	48.49	Rosettes
	32.834	0.117	(020)	43.18	Rosettes
	42.582	0.118	(401)	33.01	Rosettes
	43.983	0.119	(410)	31.69	Rosettes
Vibrated at 8 Hz with 10 ppm acetic acid	19.974	0.141	(200)	58.90	Rosettes
	25.855	0.136	(210)	47.18	Rosettes
	28.751	0.133	(211)	43.38	Rosettes
	32.838	0.131	(020)	38.56	Rosettes
	42.591	0.127	(401)	30.67	Rosettes
	43.991	0.127	(410)	29.69	Rosettes
Vibrated at 8 Hz with 10 ppm tartaric acid	19.970	0.147	(200)	56.51	Rosettes
	25.849	0.138	(210)	46.50	Rosettes
	28.744	0.135	(211)	42.75	Rosettes
	32.833	0.13	(020)	38.86	Rosettes
	42.577	0.123	(401)	31.68	Rosettes
	43.978	0.122	(410)	30.92	Rosettes
Vibrated at 8 Hz with 10 ppm formic acid	19.978	0.121	(200)	68.62	Rosettes
	25.490	0.117	(210)	55.62	Rosettes
	28.745	0.116	(211)	49.75	Rosettes
	32.822	0.112	(020)	45.13	Rosettes
	42.588	0.116	(401)	33.58	Rosettes
	43.986	0.117	(410)	32.23	Rosettes
Vibrated at 8 Hz with 10 ppm oxalic acid	19.969	0.125	(200)	66.46	Rosettes
	25.845	0.124	(210)	51.76	Rosettes
	28.745	0.124	(211)	46.54	Rosettes
	32.829	0.125	(020)	40.42	Rosettes
	42.580	0.13	(401)	29.97	Rosettes
	43.979	0.131	(410)	28.79	Rosettes

CONCLUSION

The innovative experiments were successfully demonstrated to simulate barite morphology formed from the chemistry solution induced by mechanical vibration and the presence of acids. The XRD relative intensities of each crystal face (*hkl*) of barite did not change significantly, whereas the barite crystallite size of crystal faces decreased and varied with the concentration of acids. At the same time, average rosette-like large crystals transformed into granular nanocrystals. Also, the particular crystal faces correspond to the direction of crystal growth. The morphology of barite was influenced by the mechanical

vibration and the presence of acid. One distinct morphology provided by the experiments is rosette crystal was precipitated at 50 ^{O}C with or without acid additives under the influence of vibration. The homogenous particle size of the barite may be precipitated from the induced flow vibration.

ACKNOWLEDGEMENT

This study was supported by Universitas Pembangunan Veteran, Jawa Timur, and Directorate General of Resources for Science, Technology & Higher Education, Ministry of Research, Technology and Higher Education (DIKTI) Indonesia under Doctoral Research Grant Program for the year of 2018-2019.

REFERENCES

1. S.M. Bonny and B. Jones, *Sedimentary Geology,* **203**, 36(2008), **DOI:**10.1016/j.sedgeo.2007.10.003
2. D.L. Huston and G.A Logan, *Earth and Planetary Science Letters,* **220**, 41(2004), **DOI:**10.1016/S0012-821X(04)00034-2
3. M.E. Sanz-Montero; J.P. Rodriguez-Aranda; M.A. Garcia del Cura, *Sedimentary Geology,* **222**, 138 (2009), **DOI:**10.1016/j.sedgeo.2007.10.003
4. K.S.Sorbie and E.J Mackay, *Journal of Petroleum Science and Engineering,* **27**, 85(2000), **DOI:**10.1016/S0920-4105(00)00050-4
5. J. Dymond, E. Suess and M. Lyle. *Paleoceanography and Paleoclimatology,* **7**, 163(1992), **DOI:**10.1029/92PA00181
6. J. McManus, W.M., Berelson, D.E. Hammond and G.P. Klinkhammer, *Paleoceanography and Paleoclimatology,* **14**, 53(1999), **DOI:**10.1029/1998PA900007
7. M.A. Bertram and J.P. Cowen, *Journal of Marine Research,* **55**, 577(1997), **DOI:**10.1357/0022240973224292
8. E.M Griffith and A. Paytan, *Sedimentology,* **59**, 1817(2012), **DOI:**10.1111/j.1365-3091.2012.01327.x
9. J.W. Jamieson, M.D. Hannington, M.K. Tivey, T. Hansten and N.M.B. Williamson, *Geochimica et Cosmochimica Acta,* **173**, 64(2016), **DOI:**10.1016/j.gca.2015.10.021
10. D. London, *Mineralogy Record,* **39**, 277 (2008)
11. D. Ray, D. Kota, P. Das, L. Surya Prakash and V.D. Khedekar, *Acta Geology Sinica,* **88,** 213(2014), **DOI:**10.1111/1755-6724.12192
12. H.F. Han, X. Zhu, H. Wen, C. Zhao and F. Xiao, *Ore Geology Reviews,* **86**, 297(2017), **DOI:**10.1016/j.oregeorev.2017.02.030
13. R. Hofmann and A. Baumann, *Neues Jahrbuch für Geologie und Paläontologie. Monatshefte,* **10,** 591 (1986)
14. B.S. Fu, P. Aharon, G.R. Byerly and H.H. Roberts, *Geo-Marine Letter,* **14**, 81(1994), **DOI:**10.1007/BF01203718
15. R.M. Haymon and M. Kastner, *Earth and Planetary Science Letters,* **53**, 363(1981), **DOI:**10.1016/0012-821X(81)90041-8
16. A. Paytan, S.Mearon, K. Cobb and M. Kastner, *Geology,* **30**, 747(2002), **DOI:**10.1130/0091-7613(2002)030<0747:OOMBDS>2.0.CO;2
17. J.-G. Breheret and H.J. Brumsack, *Sedimentary Geology,* **130**, 205(2000), **DOI:**10.1016/S0037-0738(99)00112-8
18. I.H. Widanagamage, A.R. Waldron and M Glamoclija. *Minerals,* **8**, **480**(2018), **DOI:**10.3390/min8110480
19. I.H. Widanagamage, E.M. Griffith, D.M. Singer, H.D. Scher, W.P. Buckley and J.M. Senko, *Chemical Geology,* **411**, 215(2015), **DOI:**10.1016/j.chemgeo.2015.07.011
20. Ö. Doğan, E. Akyol and M. Öner. *Crystal Research and Technology,* **39**, 1108(2004), **DOI:**10.1002/crat.200410297
21. E. Akyol, A. Bozkurt and M. Öner. *Polymers for Advanced Technologies*, **17**, 58(2006), **DOI:**10.1002/pat.693
22. F. Jones, P. Jones, M.I. Ogdena, W.R. Richmond, A.L. Rohl and M. Saunders. *Journal of Colloid and Interface Science*, **316**, 553(2007), **DOI:**10.1016/j.jcis.2007.09.005

23. A.J.B. Hennessy and G.M Graham. *Journal of Crystal Growth,* **237-239**, 2153(2002), **DOI:**10.1016/S0022-0248(01)02258-8
24. E. Akyol, M. Öner. *Journal of Crystal Growth*, **307**, 137(2007), **DOI:**10.1016/j.jcrysgro.2007.06.014
25. J. Nyvlt and J. Ulrich. Admixtures in Crystallization, VCH Weinheim 1995.
26. E. Akyol, M. Öner, E. Barouda and K.D Demadis. *Crystal Growth and Design*, **9**, 5145(2009), **DOI:**10.1021/cg9005423
27. M. Kowacz, C.V. Putnis and A. Putnis, *Geochimica et Cosmochimica Acta,* **71**, 5168(2007), **DOI:**10.1016/j.gca.2007.09.008
28. N. Shikazono, *Geochimica et Cosmochimica Acta,* **58**, 2203(1994), **DOI:**10.1016/0016-7037(94)90005-1
29. M. Boon and F. Jones, *Crystal Growth and Design,* **16**, 4646 (2016), **DOI:**10.1021/acs.cgd.6b00729
30. F. Jones, A. Olivera, G.M. Parkinson, A.L. Rohl, A. Stanley and T.J. Upson, *Journal of Crystal Growth,* **262**, 572 (2004), **DOI:**10.1016/j.jcrysgro.2003.10.069
31. B. Judat and M. Kind, *Journal of Colloid and Interface Science,* **269**, 341(2004), **DOI:**10.1016/j.jcis.2003.07.047
32. D.C.Y.Wong, Z. Jaworski and A.W. Nienow, *Chemical Engineering Science,* **6**, 727(2001), **DOI:**10.1016/S0009-2509(00)00282-7
33. I.H. Widanagamage, E.A. Schauble, H.D. Scher and E.M. Griffith, *Geochimica et Cosmochimica Acta,* **140**, 58 (2014), **DOI:**10.1016/j.gca.2014.10.004
34. F. Jones, P. Jones, M.I. Ogden. W.R. Richmond, A.L. Rhol and M. Saunders, *Journal of Colloid and Interface Science,* **316**, 553(2007), **DOI:**10.1016/j.jcis.2007.09.005
35. C.A.J. Appleo and D. Postma, Geochemistry, Groundwater and Pollution, 2nd ed.; CRC Press: Boca Raton, FL, USA, pp.152–154 (2005)
36. A.J.B. Hennessy and G.M. Graham, *Journal of Crystal Growth,* **237–239**, 2153(2002), **DOI:**10.1016/S0022-0248(01)02258-8
37. E. Smith, J. Hamilton, T. Davison, N.J. Fullwood and M. McGrath, *Chemical Geology,* **207,** 81 (2004), **DOI:**10.1016/j.chemgeo.2004.02.005
38. J. Benton, I.R. Collins, I. Grimsey, G.M. Parkinson and S. Rodger, *Farady Discussions,* **95**, 281(1993)
39. S.R. Freeman, F. Jones, A.O. Ogden and W.R. Richmand. *Crystal Growth & Design,* **6**, 2579 (2006), **DOI:**10.1021/cg060186z
40. N. Karaman, W. Mangestiyono, S. Muryanto, J. Jamari and A. P. Bayuseno. *Rasayan Journal of Chemistry,* **12(4)**, 1734 (2019), **DOI:**10.31788/RJC.2019.1245380
41. P. Glynn, *Reviews in Mineralogy and Geochemistry,* **40**, 481 (2000), **DOI:**10.2138/rmg.2000.40.10
42. R. Jenkins and R.L. Snyder. Introduction to X-ray powder diffractometry. London: Wiley; (1996)
43. M. Hong, J. Xu and H.H. Teng. *Geochimica et Cosmochimica Acta,* **172**, 55(2016), **DOI:**10.1016/j.gca.2014.10.004
44. A.P. Bayuseno and W.W. Schmahl, *Journal of Crystal Growth,* **498**, 336(2018), **DOI:**10.1016/j.jcrysgro.2018.06.026

[RJC-5892/2020]